Delayed wound repair and impaired angiogenesis in mice lacking syndecan-4

Rapid Publication

Frank Echtermeyer, Michael Streit, Sarah Wilcox-Adelman, Stefania Saoncella, Fabienne Denhez, Michael Detmar, and Paul F. Goetinck

Cutaneous Biology Research Center, Massachusetts General Hospital, Harvard Medical School, Charlestown, Massachusetts, USA

Address correspondence to: Paul F. Goetinck, Cutaneous Biology Research Center, MGH-East, Building 149, 13th Street, Charlestown, Massachusetts 02129, USA. Phone: (617) 726-4183; Fax: (617) 726-4189; E-mail: paul.goetinck@cbrc2.mgh.harvard.edu.

Frank Echtermeyer's present address is: Institut für Physiologische Chemie und Pathobiochemie, Westfälische-Wilhelms-Universität Münster, Münster, Germany.

Frank Echtermeyer and Michael Streit contributed equally to this work.

Received for publication June 12, 2000, and accepted in revised form December 8, 2000.

The syndecans make up a family of transmembrane heparan sulfate proteoglycans that act as coreceptors with integrins and growth factor tyrosine kinase receptors. Syndecan-4 is upregulated in skin dermis after wounding, and, in cultured fibroblasts adherent to the ECM protein fibronectin, this proteoglycan signals cooperatively with β_1 integrins. In this study, we generated mice in which the *syndecan-4* gene was disrupted by homologous recombination in embryonic stem cells to test the hypothesis that syndecan-4 contributes to wound repair. Mice heterozygous or homozygous for the disrupted *syndecan-4* gene are viable, fertile, and macroscopically indistinguishable from wild-type littermates. Compared with wild-type littermates, mice heterozygous or homozygous for the disrupted gene have statistically significant delayed healing of skin wounds and impaired angiogenesis in the granulation tissue. These results indicate that syndecan-4 is an important cell-surface receptor in wound healing and angiogenesis and that *syndecan-4* is haplo-insufficient in these processes.

J. Clin. Invest. **107**:R9–R14 (2001).

Introduction

After skin injury, a dynamic process of tissue repair commences that consists of an inflammatory response followed by re-epithelialization of the wound area and establishment of the granulation tissue with accompanying neovascularization and wound contraction (1). The entire repair process is coordinated by highly regulated interactions of cells with their surrounding ECM and from their response to growth factors. Alterations in the composition of the ECM (2, 3) or growth factors (4) can affect the wound healing process. In vitro, cells interact with the ECM molecule fibronectin through two types of cell-surface receptors: β_1 integrins (5–7) and the transmembrane heparan sulfate proteoglycan (HSPG) syndecan-4 (8, 9). Although cell adhesion to fibronectin is primarily dependent on β_1 integrins (5, 6) that interact with the cell-binding domain of this ECM molecule, cooperative signaling from syndecan-4, as a result of an interaction with the heparin-binding domain of fibronectin, leads to the assembly of focal adhesions and actin stress fibers (10).

Syndecan-4 is detectable in the epidermis, but not in the dermis, of uninjured adult mouse skin. After skin injury, however, syndecan-4 is upregulated throughout the granulation tissue on endothelial cells and fibroblasts (11, 12). Keratinocytes that migrate across the fibrin clot have reduced levels of syndecan-4 compared with the hyperproliferative keratinocytes distal from the wound edge (12).

The critical role of syndecan-4 during cell-ECM interactions in vitro (10, 13, 14), and its upregulation in the dermis of skin wounds (11, 12), suggested that syndecan-4 may play an important role in wound repair. We tested this hypothesis by generating mice in which the *syndecan-4* gene was disrupted by homologous recombination in embryonic stem (ES) cells. We find that mice homozygous or heterozygous for the disrupted *syndecan-4* gene have statistically significant delayed healing of skin wounds and impaired angiogenesis in the granulation tissue compared with wild-type littermates.

Methods

Construction of the syndecan-4 targeting vector. A 120-kb genomic clone was isolated from a 129/SVJ BAC library by hybridization with the complete murine syndecan-4 cDNA. The IRESβgeo cassette was excised from the GT1.8 IRESβgeo plasmid (15) with SalI, the ends filled with Klenow polymerase, and cloned blunt end into the NruI digested PsLII80. A 4.5-kb genomic EcoRV/BamHI fragment containing exon 5 was cloned blunt end into the SnaBI site 3′ of the IRESβgeo cassette. A 6.4-kb SacI fragment from the first intron was blunt ended by T4 polymerase and cloned into the blunt ended XhoI site located 5′ of the IRESβgeo cassette. The orientation of all cloned fragments was verified by restriction digest analysis.

Embryonic stem cells and generation of homozygous mice. Twenty million 129/J1 ES cells were electroporated with 25 μg/ml of SpeI linearized targeting vector and subjected to G418 selection (16). G418-resistant clones were screened for homologous recombination of the *syndecan-4* locus by Southern blot hybridization. Two recombinant clones were expanded, reanalyzed by Southern blot hybridiza-

tion, and injected into C57BL/6 blastocysts. Chimeric male founder mice were backcrossed to C57BL/6 females, and heterozygous offsprings were backcrossed on that background for at least four generations. Genotype analysis was performed by Southern blot hybridization on genomic DNA isolated from tails.

Isolation of dermal fibroblasts. Primary skin fibroblasts were isolated from newborn *syndecan-4*$^{+/+}$, *syndecan-4*$^{+/-}$, and *syndecan-4*$^{-/-}$ mice from the same litter. Mice were sacrificed, and their skins were removed, flattened, and floated on a 0.25% trypsin solution (Life Technologies Inc., Gaithersburg, Maryland, USA) at 4°C overnight. The dermis was separated from the epidermis and dissociated by stirring at room temperature for 30 minutes in HBSS containing collagenase (500 μg/ml) (Life Technologies Inc.). The cell suspension of each skin was passed through a cell strainer (Becton Dickinson and Co., Franklin Lakes, New Jersey, USA) and transferred to a 10-cm cell culture dish and cultured as described previously (10). Dermal fibroblasts were maintained at subconfluent densities and used between passages three and six.

RT-PCR. RT-PCR was performed on 1 μg of total RNA from *syndecan-4*$^{+/+}$, *syndecan-4*$^{+/-}$, and *syndecan-4*$^{-/-}$ fibroblasts as described elsewhere (10). PCR reactions were performed with primers specific for syndecan-4 (forward: nucleotide [NT] +76 to NT +100 and reverse: NT +588 to +609), β-actin (forward: NT +73 to NT +85 and reverse: NT +993 to NT +1006), and GAPDH (CLONTECH Laboratories Inc., Palo Alto, California, USA). Bands were analyzed on 1.5% agarose gel, visualized by ultraviolet activation of incorporated ethidium bromide, and photographed.

Flow cytometry. Analysis of surface expression of syndecan-4 and the integrin β_1 chain was performed as described previously (10) using affinity-purified anti-mouse syndecan-4 antibodies (MS-4-E) and a rat mAb directed against the mouse β_1 integrin chain (9EG7).

Wound healing studies. Four excisional full-thickness wounds were made with 6-mm skin biopsy punches on the backs of three groups of five 10-week-old female mice that were either *syndecan-4*$^{+/+}$, *syndecan-4*$^{+/-}$, or *syndecan-4*$^{-/-}$. Wound closure was monitored daily as described elsewhere (3). Area measurements were made using the IP-LAB software (Scanalytics, Fairfax, Virginia, USA). Histological analysis of the wounds was performed on mice that were sacrificed at 3 and 7 days after wounding. In a separate experiment, wounds were created on eight 10-week-old female mice of each of the three genotypes, and the skins were collected at 6 days after wounding for the analysis of blood vessels. Statistical analysis was performed using the unpaired Student's *t* test.

Histology and immunocytochemistry. Tissues were fixed in 4% paraformaldehyde for 2 hours and embedded in paraffin. Staining with hematoxylin and eosin was done on 6-μm paraffin sections. Blood vessels were analyzed on 6-μm cryostat sections stained with an mAb against mouse CD31 (PECAM-1) (PharMingen, San Diego, California, USA) as described elsewhere (17). Image analysis was performed as described previously (3), and the number of vessels, average vessel size, and total vessel area were determined. Statistical analysis was performed using the unpaired Student's *t* test. The assembly of focal adhesions and actin stress fibers was assessed by confocal microscopic analysis of vinculin and actin stress fibers in fibroblasts adherent to fibronectin for 3 hours in the presence of 10% FBS (10).

In vitro wound healing models. Primary fibroblast cultures were established for 2 days in DMEM with 10% FBS followed by an overnight culture in DMEM with 2% FBS. In vitro wound closure tests were performed by creating clear lines in confluent cultures with a sterile yellow plastic pipette tip. After two washes with medium, the monolayers were covered with fresh medium and the migration of the cells into the cleared spaces was monitored over time. The control medium used during wound closure was DMEM with 2% FBS. This medium was supplemented with either 25 ng/ml of FGF-2 (R&D Systems Inc., Minneapolis, Minneapolis, USA) or 25 ng/ml of EGF (Becton Dickinson and Co.).

In vitro wound contraction assays (18) were done by allowing 2 ml of DMEM with 10% FBS, 1.0 mg/ml of bovine type I collagen (Vitrogen 100; Collagen Corp., Palo Alto, California, USA) and 6.7×10^4 fibroblasts to form a gel in 35-mm dishes for 3 hours at 37°C before releasing the gels from the dish. Skin fibroblast populations were derived from four *syndecan-4*$^{+/+}$, seven *syndecan-4*$^{+/-}$, and three *syndecan-4*$^{-/-}$ newborn mice. Assays were performed in triplicate for each of the 14 different fibroblast populations. Gel contraction was quantified by measuring the diameter of the floating gels.

Results

Establishment of syndecan-4–deficient mice. Of 200 clones selected, 38 were screened by Southern blot hybridization of genomic DNA digested with SpeI and EcoRV using the 5′ external probe indicated in Figure 1a. Of these, 17 clones were determined to carry the recombinant *syndecan-4* allele (synd-4^{tm1Goe}) based on the presence of predicted 12-kb recombinant and 14-kb wild-type allele fragments (Figure 1b). Two clones (13 and 27) were expanded, reanalyzed by Southern blot hybridization, and injected into C57BL/6 blastocysts. Chimeric male founder mice were backcrossed to C57BL/6 females, and the genotype of carriers of the recombinant allele were identified by Southern blot hybridization (Figure 1c) and/or PCR analysis on genomic DNA isolated from tails. Mice homozygous and heterozygous for the disrupted *syndecan-4* core protein gene develop normally, are fertile, and show no overt morphological defects. The mutant *syndecan-4* gene segregated in a normal mendelian fashion, yielding approximately 25% homozygous mutant offspring in matings between mice heterozygous for the recombinant allele.

Syndecan-4 is absent in syndecan-4$^{-/-}$ *mice*. RT-PCR analysis of mRNA from skin fibroblasts obtained from 1-day-old sibling offspring of heterozygous parents revealed that a 524-bp syndecan-4–specific band could be amplified from *syndecan-4*$^{+/+}$ and *syndecan-4*$^{+/-}$ cells but not from *syndecan-4*$^{-/-}$ cells. The predicted 946-bp β-actin and 983-bp GAPDH bands were amplified

Figure 1
Generation and characterization of *syndecan-4* recombinant mice. (**a**) Structure of the murine *syndecan-4* gene, the targeting vector, and the targeted allele. Exons are numbered 1 through 5. This organization is similar to that reported by others (25). Sa, SacI; Sp, SpeI; Av, AvrII; EV, EcoRV; B, BamHI; Xh, XhoI; Sn, SnaBI. SA, splice acceptor; IRES, internal ribosomal entry site; LACZ, β-galactosidase; NEO, neomycin resistance. (**b**) Southern blot analysis of ES clones. (**c**) Southern blot analysis of mice derived from matings between *syndecan-4*$^{+/-}$ mice. Wild-type (14.1 kb) and targeted alleles (12 kb) are detected with the 5′ probe. (**d**) RT-PCR of mRNA results in a syndecan-4–specific 524-bp band from *syndecan-4*$^{+/+}$ and *syndecan-4*$^{+/-}$ cells but not from *syndecan-4*$^{-/-}$ cells. mRNA for both β-actin and GAPDH is present in extracts of cells of all three genotypes. (**e**) Flow cytometric analysis of cell-surface syndecan-4 on skin fibroblasts. Syndecan-4 (Synd-4) is detected on *syndecan-4*$^{+/+}$ cells (upper left) but not on *syndecan-4*$^{-/-}$ cells (upper right). β_1 Integrins (β_1) are expressed on cells of both genotypes (lower panels). Secondary antibodies alone were used as control (Cont).

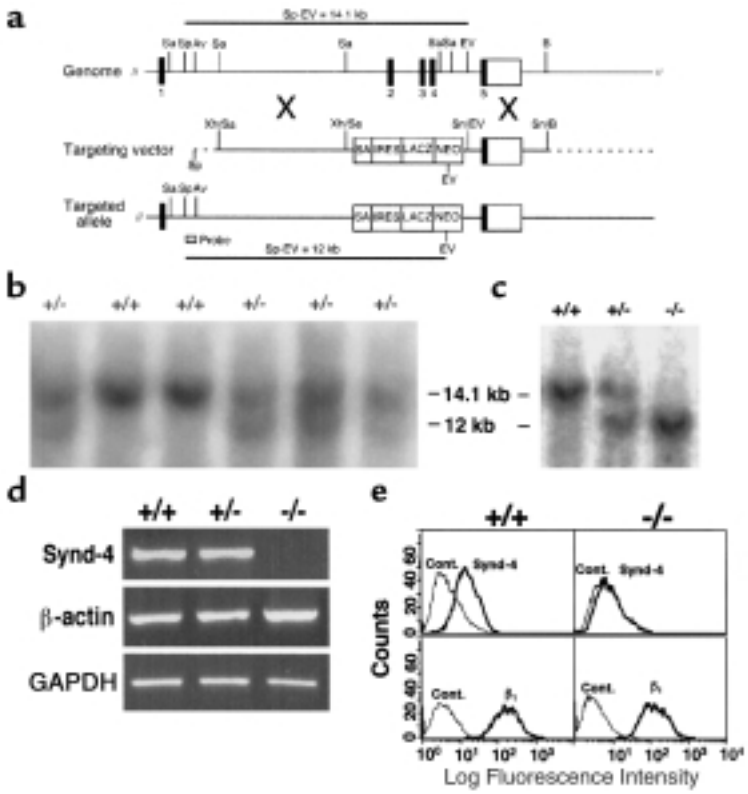

from mRNA isolated from cells of all three genotypes (Figure 1d). A shift in fluorescence intensity for the *syndecan-4*$^{+/+}$ cells (Figure 1e, upper left) with the anti–syndecan-4 antibodies indicates the presence of syndecan-4 on these cells. The absence of a shift with the *syndecan-4*$^{-/-}$ cells (Figure 1e, upper right) indicates an absence of syndecan-4 on these cells, confirming that the *syndecan-4* gene had been disrupted. Both the *syndecan-4*$^{+/+}$ (Figure 1e, lower left) and *syndecan-4*$^{-/-}$ (Figure 1e, lower right) cells show an identical shift in fluorescence intensity with the anti-β_1 antibodies.

Impaired wound healing in syndecan-4$^{-/-}$ *and syndecan-4*$^{+/-}$ *mice*. Excisional wounds were made on the backs of five 10-week-old female mice of each of the three genotypes. The wound areas of the of *syndecan-4*$^{+/+}$ mice were reduced by more than 50% within 2 days and up to 75% within 4 days after wounding. In contrast, both *syndecan-4*$^{-/-}$ and *syndecan-4*$^{+/-}$ mice showed a delay in the rate of wound healing compared with *syndecan-4*$^{+/+}$ mice during the first 7 days after wounding (Figure 2). These differences were statistically significant between days 3 and 6 after wounding. By day 9, all mice had closed their wounds to the same extent of about 80%. Complete wound closure in mice of all three genotypes was evident by day 12 (data not shown).

Day 3 after wounding was the first time point at which a statistically significant delay in the closure of the wounds of *syndecan-4*$^{-/-}$ and *syndecan-4*$^{+/-}$ mice was apparent. At this time point, comparable re-epithelialization had started at the edge of the wounds of the *syndecan-4*$^{+/+}$ and *syndecan-4*$^{-/-}$ mice (Figure 3, double arrows) as well as in the *syndecan-4*$^{+/-}$ mice (data not shown). After 5 to 7 days, the new epidermis had formed completely and no differences were evident between the three genotypes. At 3 days, in the dermis of *syndecan-4*$^{+/+}$ mice, there was an increase in the granulation tissue at the edge of the wound bed and the wounds of the *syndecan-4*$^{+/+}$ mice had contracted (Figure 3a, left panels). In contrast, the wounds of the *syndecan-4*$^{-/-}$ (Figure 3a, right panels) and *syndecan-4*$^{+/-}$ (data not shown) mice showed a greatly reduced accumulation of granulation tissue at the wound edge with a thin granulation tissue layer covering the wound bed. Unlike the wounds of the *syndecan-4*$^{+/+}$ mice, those of the *syndecan-4*$^{-/-}$ and *syndecan-4*$^{+/-}$ mice did not contract at this time. By day 7, the wound bed was completely filled with granulation tissue in the dermis of all three genotypes, but the granulation tissue in the wounds of the *syndecan-4*$^{+/+}$ mice seemed more vascularized

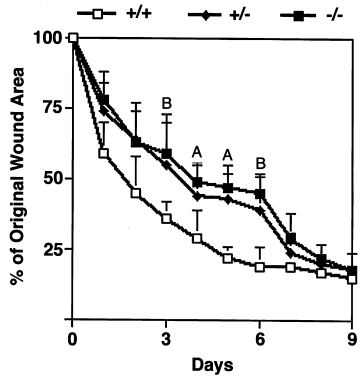

Figure 2
Delayed wound healing in mice homozygous (–/–) or heterozygous (+/–) for the recombinant *syndecan-4* allele compared with wild-type (+/+) littermates. A statistically significant delay is seen between days 3 and 6 after wounding. Data are expressed as means ± SEM (n = 20). $^{A}P < 0.05$. $^{B}P < 0.01$.

Figure 3
(**a**) Histological analysis of wound healing in *syndecan-4*$^{+/+}$ (left panels) and *syndecan-4*$^{-/-}$ (right panels) mice at 3 days after wounding. The higher magnification in the bottom panels is of the region in the upper right edge of the wounds in the respective top panels. Double arrows: margin of epithelium; single arrow: blood vessel in dense granulation tissue (arrowheads); solid lines in bottom panels: wound edge. Bar, 200 μm. (**b**) Immunohistochemical examination of wounds 6 days after wounding for the endothelial cell marker CD31 in *syndecan-4*$^{+/+}$ (left) and in *syndecan-4*$^{-/-}$ (right) mice. Bar, 100 μm. (**c**) Quantitative analysis of angiogenesis. The numbers of vessels per unit area are the same for the three genotypes (left). Average vessel size (middle) and total vessel area (right) in the wounds of *syndecan-4*$^{-/-}$ or *syndecan-4*$^{+/-}$ mice are significantly different from those of *syndecan-4*$^{+/+}$ mice. Data are expressed as means ± SEM (n = 8). $^{A}P < 0.05$.

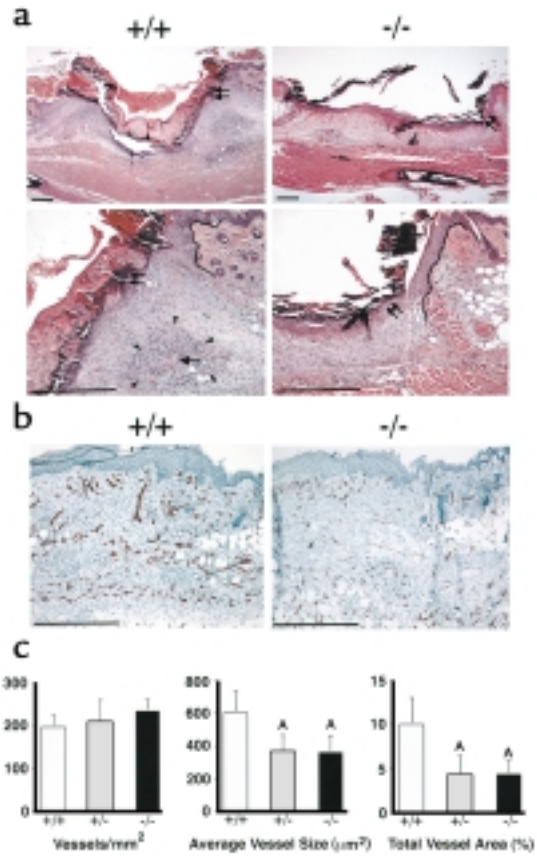

than in those of the *syndecan-4*$^{-/-}$ and *syndecan-4*$^{+/-}$ mice (data not shown).

Impaired angiogenesis in syndecan-4$^{-/-}$ *and syndecan-4*$^{+/-}$ *mice*. To quantify the differences in wound vascularization of the granulation tissues, eight female mice of each of the three genotypes were wounded and examined 6 days after wounding for the endothelial specific marker CD31. The immunohistological micrographs show greater staining for CD31 in the granulation tissue of *syndecan-4*$^{+/+}$ mice (Figure 3b, left) compared with *syndecan-4*$^{-/-}$ (Figure 3b, right) and *syndecan-4*$^{+/-}$ (data not shown) mice. The number of vessels per unit area was comparable in the wounds of the three genotypes (Figure 3c, left). However, a statistically significant reduction ($P < 0.05$) of the average vessel size in the granulation tissue of the *syndecan-4*$^{-/-}$ and *syndecan-4*$^{+/-}$ mice (Figure 3c, middle) is evident. The smaller vessel size results in a statistically significant reduction in the relative wound area occupied by blood vessels, i.e., the total vessel area, for both *syndecan-4*$^{-/-}$ and *syndecan-4*$^{+/-}$ mice (Figure 3c, right).

In vitro analyses of primary skin fibroblasts. Dermal skin fibroblasts, of all three genotypes, adherent to fibronectin spread and assemble an actin cytoskeleton and vinculin containing adhesion sites similar to those shown by Ishiguro et al. (19) for whole embryo derived fibroblasts (data not shown).

In vitro wound migration assays reveal a slower rate of cell migration by the *syndecan-4*$^{-/-}$ fibroblasts compared with the *syndecan-4*$^{+/+}$ or *syndecan-4*$^{+/-}$ fibroblasts cultured in DMEM containing 2% FBS. The *syndecan-4*$^{+/+}$ or *syndecan-4*$^{+/-}$ fibroblasts had closed the wounds by 23 hours, whereas the *syndecan-4*$^{-/-}$ fibroblasts had not (Figure 4, control). No differences were observed between *syndecan-4*$^{+/+}$ and *syndecan-4*$^{+/-}$ fibroblasts. Supplementing the medium with either 25 ng/ml of FGF-2 (Figure 4, FGF-2) or with 25 ng/ml of EGF (Figure 4, EGF) did not alter the rate of wound closure by cells of any of the three genotypes.

The gel contraction assays reveal no differences for the three genotypes in their ability to contract collagen gels. The percent contraction of the gels (mean ± SEM) at the end of 3 days was 75.12 ± 10.96 (n = 4), 79.21 ± 7.37 (n = 7), and 85.33 ± 10.66 (n = 3) for the *syndecan-4*$^{+/+}$, *syndecan-4*$^{+/-}$, and *syndecan-4*$^{-/-}$ fibroblasts, respectively. Student t tests indicate that these values are not statistically different from each other.

Discussion

The results presented in this study clearly support the hypothesis that syndecan-4 plays a role in wound healing and angiogenesis and that syndecan-4 is haplo-insufficient for both of these processes. The involvement of syndecan-4 in wound healing and angiogenesis is consistent with the observation that syndecan-4 is upregulated in both fibroblasts and endothelial cells of the granulation tissue after skin injury (11, 12).

Wound healing is a dynamic process in which the behavior of cells is influenced both by their interactions with the ECM and by their response to growth factors (1). Because syndecans function as coreceptors for both insoluble ligands such as components of the ECM and soluble ligands such as growth factors (20), the observed delay in wound healing in *syndecan-4*$^{-/-}$ and *syndecan-4*$^{+/-}$ mice could result from an impairment of either or both of these functions. The reduced rate of migration of *syndecan-4*$^{-/-}$ fibroblasts in the in vitro wound healing model suggests that altered cell-matrix interactions could contribute to the delayed excisional wound healing. However, it seems that the in vitro model only represents part of a more complex mechanism, as the *syndecan-4*$^{+/-}$ fibroblasts behave like wild-type cells in vitro, whereas in vivo, the *syndecan-4*$^{+/-}$ animals display the same impaired wound healing and angiogenesis as do the null mice. The collagen gel contraction assay also suggests a complex situation. This assay has been described as an in vitro

Figure 4
In vitro migration analysis of *syndecan-4* recombinant fibroblasts. Wild-type and heterozygous fibroblasts fill in a space created in an in vitro wound healing model completely by 23 hours in contrast to *syndecan-4*$^{-/-}$ cells. Fibroblasts were grown to confluency in 10% FBS and then placed in 2% FBS overnight. The in vitro wound assays were performed on cultures of all three genotypes in control medium (DMEM containing 2% FBS) or medium supplemented with 25 ng/ml of FGF-2 or 25 ng/ml of EGF. The wound closure was monitored over time and terminated upon complete closure of the wounds by the *syndecan-4*$^{+/+}$ fibroblasts.

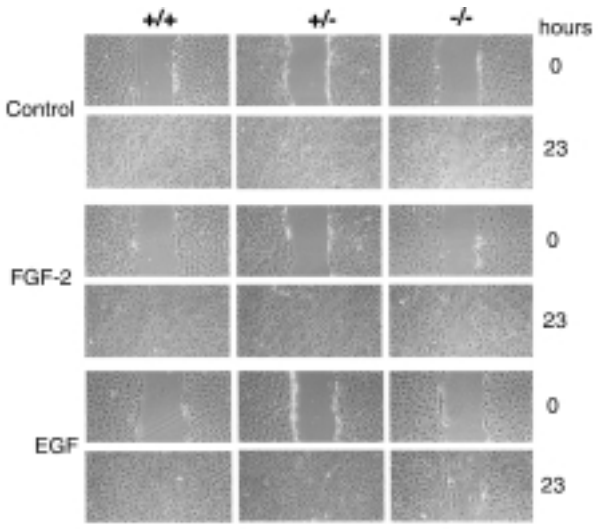

model for predicting the rate of wound closure (18). We found no correlation between fibroblasts isolated from the three genotypes and their ability to contract collagen gels. A lack of correlation between collagen gel contraction assays and wound closure has also been reported for mice null for the thrombospondin-2 gene. These mice have an accelerated wound closure (2), yet fibroblasts from the null mice do not contract collagen gels efficiently (21).

The cellular basis for the slower migration of *syndecan-4*$^{-/-}$ fibroblasts in vitro is not obvious from the analysis of their ability to assemble focal adhesions and actin stress fibers in vitro. Syndecan-4 signals cooperatively with β_1 integrins in the assembly of actin stress fibers and focal adhesions (10) by ligating to the heparin-binding domain of fibronectin; yet, *syndecan-4*$^{-/-}$ fibroblasts adherent to fibronectin are indistinguishable from *syndecan-4*$^{+/+}$ cells (19). These results suggest that an unidentified receptor in *syndecan-4*$^{-/-}$ cells may interact with the heparin-binding domain of fibronectin and thus compensate for syndecan-4 deficiency in the assembly process, in agreement with Ishiguro et al. (19). Such a compensatory signaling pathway might involve another member of the syndecan family and might explain why *syndecan-4* null mice are indistinguishable from their wild-type littermates. Only under a stress situation, such as wound repair demonstrated in this study, would the role for syndecan-4 become evident.

The delayed wound repair in mice with the disrupted syndecan-4 gene could also result from alterations in the interactions of cells with growth factors such as FGF-2. FGF-2 null mice exhibit delayed wound healing (4), and interactions of FGF-2 with syndecan-4 have been demonstrated (22). For this reason, we tested for a possible role for FGF-2 in our in vitro wound closure assay and compared this heparin-binding growth factor with EGF, a growth factor that does not bind to heparin. Neither FGF-2 nor EGF had any effect on the rate of cell migration in these assays. That the fibroblasts can respond to exogenous factors is evident from the accelerated wound closure that takes place in the presence of 10% FBS instead of 2%. However, although there was an overall acceleration in wound closure, the *syndecan-4*$^{+/+}$ and the *syndecan-4*$^{+/-}$ fibroblasts still migrated faster than the *syndecan-4*$^{-/-}$ fibroblasts (our unpublished observations). We conclude, therefore, that a component of the delayed wound closure in the *syndecan-4*$^{-/-}$ mice can be attributed to decreased cell migration, but our in vitro wound assay suggests that the effect of syndecan-4 in cell migration is not dependent on interactions with FGF-2. Additionally, we have observed that primary skin fibroblasts cultured under the same conditions as described in the present study show a proliferative response to FGF-2. The magnitude of the response, however, is the same for cells of all three *syndecan-4* genotypes (our unpublished observations). This observation would suggest that the FGF-2–mediated proliferative response is also not dependent on interactions with syndecan-4.

Syndecan-1 is also upregulated during skin wound healing, but this upregulation is restricted to the endothelial cells of the granulation tissue (11, 12, 23). Lack of syndecan-1 results in delayed skin (20) and corneal wound (24) repair. Like *syndecan-4* null mice, *syndecan-1* null mice are viable and fertile. It is tempting to speculate that syndecan-4 and syndecan-1 might provide complementary signaling pathways during wound healing. An analysis of mice that are null for both syndecan-4 and -1 might shed light on the role of these two HSPGs in wound healing.

Acknowledgments

The authors thank En Li for advice in the generation of the syndecan-4 null mice. This work was supported in part by NIH/NICHD grant HD-37490 (to P.F. Goetinck), by NIH/NCI grants CA69184 and CA86410 to Michael Detmar, and by the Cutaneous Biology Research Center through the MGH/Shiseido Company agreement (to P.F. Goetinck and Michael Detmar); F. Echtermeyer was supported by Research Fellowship EC 178/2 from the Deutsche Forschungsgemeinschaft and by a Schering Laboratories Dermatology Foundation Research Fellowship; M. Steit was supported by a Dermatology Foundation Research

Fellowship; and S. Wilcox-Adelman was supported by NIH postdoctoral training grant T32 AR07098.

1. Clark, R.A. 1993. Biology of dermal wound repair. *Dermatol. Clin.* **11**:647–666.
2. Kyriakides, T.R., Tam, J.W.Y., and Bornstein, P. 1999. Accelerated wound healing in mice with a disruption of the thrombospondin 2 gene. *J. Invest. Dermatol.* **113**:782–787.
3. Streit, M., et al. 2000. Thrombospondin-1 suppresses wound healing and granulation tissue formation in the skin of transgenic mice. *EMBO J.* **19**:3272–3282.
4. Ortega, S., Ittmann, M., Tsang, S.H., Ehrlich, M., and Basilico, C. 1998. Neuronal defects and delayed wound healing in mice lacking fibroblast growth factor 2. *Proc. Natl. Acad. Sci. USA.* **95**:5672–5677.
5. Burridge, K., and Chrzanowska-Wodnicka, M. 1996. Focal adhesions, contractility, and signaling. *Annu. Rev. Cell Dev. Biol.* **12**:463–518.
6. Schoenwaelder, S.M., and Burridge, K. 1999. Bidirectional signaling between the cytoskeleton and integrins. *Curr. Opin. Cell Biol.* **11**:274–286.
7. Clark, E.A., and Brugge, J.S. 1995. Integrins and signal transduction pathways: the road taken. *Science.* **268**:233–239.
8. Woods, A., and Couchman, J.R. 1994. Syndecan 4 heparan sulfate proteoglycan is a selectively enriched and widespread focal adhesion component. *Mol. Biol. Cell.* **5**:183–192.
9. Baciu, P.C., and Goetinck, P.F. 1995. Protein kinase C regulates the recruitment of syndecan-4 into focal contacts. *Mol. Biol. Cell.* **6**:1503–1513.
10. Saoncella, S., et al. 1999. Syndecan-4 signals cooperatively with integrins in a Rho-dependent manner in the assembly of focal adhesions and actin stress fibers. *Proc. Natl. Acad. Sci. USA.* **96**:2805–2810.
11. Gallo, R., Kim, C., Kokenyesi, R., Adzick, N.S., and Bernfield, M. 1996. Syndecans-1 and -4 are induced during wound repair of neonatal but not fetal skin. *J. Invest. Dermatol.* **107**:676–683.
12. Gallo, R.L., and Bernfield, M. 1996. *Proteoglycans and their role in wound repair.* Plenum Press. New York, New York, USA. 475–492.
13. Echtermeyer, F., Baciu, P.C., Saoncella, S., Ge, Y., and Goetinck, P.F. 1999. Syndecan-4 core protein is sufficient for the assembly of focal adhesions and actin stress fibers. *J. Cell Sci.* **112**:3433–3441.
14. Longley, R.L., et al. 1999. Control of morphology, cytoskeleton and migration by syndecan-4. *J. Cell Sci.* **112**:3421–3431.
15. Mountford, P., et al. 1994. Dicistronic targeting constructs: reporters and modifiers of mammalian gene expression. *Proc. Natl. Acad. Sci. USA.* **91**:4303–4307.
16. Li, E., Bestor, T.H., and Jaenisch, R. 1992. Targeted mutation of the DNA methyltransferase gene results in embryonic lethality. *Cell.* **69**:915–926.
17. Detmar, M., et al. 2000. Expression of vascular endothelial growth factor induces an invasive phenotype in human squamous cell carcinomas. *Am. J. Pathol.* **156**:159–167.
18. Grinnell, F. 1994. Fibroblasts, myofibroblasts, and wound contraction. *J. Cell Biol.* **124**:401–404.
19. Ishiguro, K., et al. 2000. Syndecan-4 deficiency impairs focal adhesion formation only under restricted conditions. *J. Biol. Chem.* **275**:5249–5252.
20. Bernfield, M., et al. 1999. Function of cell surface heparan sulfate proteoglycans. *Annu. Rev. Biochem.* **69**:729–777.
21. Kyriakides, T.R., Zhu, Y.H., Tam, J.W.Y., Yang, Z., and Bornstein, P. 1998. Accelerated wound healing in mice with a disruption of the thrombospondin 2 gene. *Mol. Biol. Cell.* **9**:59a. (Abstr.)
22. Volk, R., Schwartz, J.J., Li, J., Rosenberg, R.D., and Simons, M. 1999. The role of syndecan cytoplasmic domain in basic fibroblast growth factor-dependent signal transduction. *J. Biol. Chem.* **274**:24417–24424.
23. Elenius, K., et al. 1991. Induced expression of syndecan in healing wounds. *J. Cell Biol.* **114**:585–595.
24. Stepp, M.A., et al. 1999. Delayed corneal wound repair in mice lacking syndecan-1. *Mol. Biol. Cell.* **10**:459a. (Abstr.)
25. Tsuzuki, S., et al. 1997. Molecular cloning, genomic organization, promoter activity, and tissue-specific expression of the mouse ryudocan gene. *J. Biochem.* **122**:17–24.